HHS Public Access

Author manuscript

Cancer Cell. Author manuscript; available in PMC 2015 April 17.

Published in final edited form as:

Cancer Cell. 2010 September 14; 18(3): 231–243. doi:10.1016/j.ccr.2010.08.007.

An ARF-independent c-Myc-activated tumor suppression pathway mediated by ribosomal protein-Mdm2 interaction

Everardo Macias[1,2], **Aiwen Jin**[1,2], **Chad Deisenroth**[1,2,4], **Krishna Bhat**[5], **Hua Mao**[3], **Mikael S. Lindström**[6], and **Yanping Zhang**[1,2,3,*]

[(1)]Department of Radiation Oncology, School of Medicine, the University of North Carolina at Chapel Hill, Chapel Hill, NC.

[(2)]Lineberger Comprehensive Cancer Center, School of Medicine, the University of North Carolina at Chapel Hill, Chapel Hill, NC.

[(3)]Department of Pharmacology, School of Medicine, the University of North Carolina at Chapel Hill, Chapel Hill, NC.

[(4)]Curriculum in Genetics and Molecular Biology, School of Medicine, the University of North Carolina at Chapel Hill, Chapel Hill, NC.

[(5)]Departments of Pathology, The University of Texas, M.D. Anderson Cancer Center, Houston, Texas.

[(6)]Department of Oncology-Pathology, Karolinska Institute, Stockholm, Sweden.

Summary

In vitro studies have shown that inhibition of ribosomal biogenesis can activate p53 through ribosomal protein (RP)-mediated suppression of Mdm2 E3 ligase activity. To study the physiological significance of the RP-Mdm2 interaction, we generated mice carrying a cancer-associated cysteine-to-phenylalanine substitution in the zinc finger of Mdm2 that disrupted its binding to RPL5 and RPL11. Mice harboring this mutation, although retain normal p53 response to DNA damage, lack p53 response to perturbations in ribosome biogenesis. Loss of RP-Mdm2 interaction significantly accelerates Eμ-*Myc* induced lymphomagenesis. Furthermore, ribosomal perturbation induced p53 response does not require tumor suppressor p19Arf. Collectively, our findings establish RP-Mdm2 interaction as a genuine p53 stress-signaling pathway activated by aberrant ribosomal biogenesis and essential for safeguarding against oncogenic c-Myc-induced tumorigenesis.

[(*)]To whom correspondence should be addressed: University of North Carolina at Chapel Hill, Department of Radiation Oncology, Chapel Hill, NC 27599-7512 Tel.: 919-966-7713, Fax.: 919-966-7681, ypzhang@med.unc.edu.

Keywords

Mdm2; p53; zinc finger; cancer; mutation; nucleolus; ribosome biogenesis; RPL11

Introduction

The p53 transcription factor interacts with a large number of proteins and plays a central role in regulating cell growth, proliferation and apoptosis (Vogelstein et al., 2000). The function of p53 is negatively controlled by Mdm2 (HDM2 in humans, henceforth as Mdm2), which itself is a transcriptional target of p53, thus constituting an auto regulatory feedback loop (Picksley and Lane, 1993). Mdm2 controls the activity of p53 and is regulated in response to a multitude of stressors, one of these stressors is the so called nucleolar stress (a.k.a. ribosomal stress) (Rubbi and Milner, 2003). Previous evidence demonstrates a nucleolar stress response to a low dose (5 nM) of Actinomycin D (Act D) (Dai and Lu, 2004; Dai et al., 2004; Jin et al., 2004), 5-Fluorouracil (5-FU) (Gilkes et al., 2006; Sun et al., 2007), serum depletion and contact inhibition (Bhat et al., 2004), mycophenolic acid (MPA)-mediated depletion of GTP (Sun et al., 2008), or interfering with nucleolar function by ectopic overexpression of nucleostemin (Dai et al., 2008). At low concentrations (e.g. <10 nM), Act D selectively inhibits ribosomal biogenesis through inhibiting pol I-dependent transcription of rRNA (Iapalucci-Espinoza and Franze-Fernandez, 1979; Perry and Kelley, 1970). 5-FU is a pyrimidine analog whose metabolite, FUTP, is extensively incorporated into RNA, disrupting normal RNA processing (Longley et al., 2003). MPA inhibits *de novo* guanine nucleotide biosynthesis, leading to depletion of intracellular guanine nucleotide and blockage of *de novo* RNA synthesis (Allison, 2005). As the prime location for ribosome biogenesis, the nucleolus is highly susceptible to perturbations in the process of ribosome assembly, thereby clarifying how nucleolar stress is often synonymous with “ribosomal stress”.

Ribosome biogenesis is an essential cellular process that involves three fundamental steps: coordinated expression of ribosomal RNA (rRNA) and ribosomal protein (RP), processing of rRNA, and assembly of the 40S and 60S ribosome subunits (Perry, 2007). Perturbation of any step in this process is thought to lead to nucleolar stress, triggering specific binding of Mdm2 to several RPs, including L11 (Fumagalli et al., 2009; Lohrum et al., 2003; Zhang et al., 2003), L23 (Dai et al., 2004; Jin et al., 2004), and L5 (Dai and Lu, 2004). Increased binding of ribosomal proteins to Mdm2 leads to p53 stability and transactivation. In addition to L5, L11, and L23, additional ribosomal proteins such as S7 (Chen et al., 2007; Zhu et al., 2009) and L26 (Ofir-Rosenfeld et al., 2008) have also been shown to interact with Mdm2. The consequence of the S7-Mdm2 interaction resembles that of the other RPs in terms of binding to Mdm2 and activation of p53. However, surprising findings show that MdmX, a homologue of Mdm2, can facilitate S7’s suppression of Mdm2 and that S7, itself a substrate for Mdm2 ubiquitination, acts as both an effector and affector of Mdm2 (Zhu et al., 2009). The interaction of L26 with Mdm2 appears to perform a different function. L26 was found to increase the translational rate of p53 mRNA through binding to its 5′ untranslated region (UTR) and in this case Mdm2 acts as an E3 ubiquitin ligase for ubiquitylation and degradation of L26, thereby inhibiting p53 translation (Ofir-Rosenfeld et al., 2008).

Collectively, these findings indicate that RPs could play a pivotal role in mediating a p53 response to nucleolar stress (reviewed in (Zhang and Lu, 2009))

Mdm2 contains three highly conserved regions: the N-terminus, the C-terminus, and the central zinc finger area. The N-terminal conserved domain is important for p53 binding. The C-terminal domain contains a RING finger essential for the E3 ubiquitin ligase function of Mdm2. The function of the central acidic domain, including a highly conserved C4 zinc finger, is not fully understood. Intriguingly, several small basic proteins that function to inhibit Mdm2, including p19Arf and each of the aforementioned ribosomal proteins, all interact with the conserved central acidic domain of Mdm2 (Figure 1A), suggesting that this region might serve as a site for receiving and integrating various Mdm2-regulatory signals into the p53 pathway (Dai et al., 2006).

Mdm2 gene amplification is the predominant mechanism ascribed to oncogenic activation and has been detected in many types of human cancers including soft tissue sarcomas (Oliner et al., 1992) and brain tumors (Corvi et al., 1995; Reifenberger et al., 1993). In addition to gene amplification and protein overexpression, mutations within the *Mdm2* gene have been reported in several types of human cancers (Schlott et al., 1997; Tamborini et al., 2001). Intriguingly, many of the cancer associated Mdm2 mutations occur at or near the central zinc finger, including point mutations altering one of the conserved zinc-coordinating cysteines and truncations around the zinc finger. *In vitro* studies have shown that mutations at the zinc-coordinating cysteine residues disrupts Mdm2 binding to L5 and L11, and as a result diminishes the capacity of Mdm2 to respond to nucleolar stress (Lindstrom et al., 2007). However, despite recent evidence from multiple laboratories corroborating a putative RP-Mdm2-p53 signaling pathway, the validity of RP mediated signaling to p53 has yet to be demonstrated *in vivo.* The current study was designed to investigate this.

Results

Generation of Mdm2^{C305F} mice

To investigate the physiological relevance of zinc finger mutation, we generated mice bearing a cancer-associated Cys-to-Phe substitution in one of the zinc-coordinating residues of Mdm2. The targeting construct, containing a C305F substitution and a new *Spe1* restriction site (Figure 1B), was recombined into the *Mdm2* locus of 129/Sv embryonic stem (ES) cells. Successful targeting of *Mdm2* allele was identified by Southern blotting of genomic DNA isolated from the ES cells (Figure 1C), and was confirmed by *Spe1* digestion of PCR-amplified genomic DNA (Figure 1D). The ES cells were microinjected into C57BL/6 blastocysts to produce chimeras. Chimera males were mated with C57BL/6 females to produce germline transmission of the Mdm2^{C305F} allele. The targeted allele was reconfirmed through direct sequencing of the genomic DNA after germline transmission was obtained (data not shown). The neomycin resistance gene *(neo)* was removed from the targeted allele by crossing *neo-Mdm2^{C305F}* heterozygous mice with transgenic mice ubiquitously expressing *Cre* recombinase. The resulting *Mdm2$^{+/C305F}$* heterozygous mice were then backcrossed with C57BL/6 mice for five generations to generate near congenic (~97% pure) C57BL/6 *Mdm2$^{+/C305F}$* mice.

Mdm2^{C305F} mice have a normal lifespan

The heterozygous *Mdm2*$^{+/C305F}$ mice were intercrossed to generate homozygous *Mdm2*$^{C305F/C305F}$ mice. Of 151 pups born from the intercross an accurate Mendelian inheritance was observed (Figure 1E). A survival study was performed to examine the effect of Mdm2^{C305F} mutation on longevity. At least 17 animals were included for each genotype, 2-4 animals of the same sex were housed in each cage, and the longevity of these mice were monitored over a 900-day period. Kaplan-Meier survival curve shows a similar survival rate among wild type, *Mdm2*$^{+/C305F}$ and *Mdm2*$^{C305F/C305F}$ mice (Figure 1F). Additionally, *Mdm2*$^{+/C305F}$ or *Mdm2*$^{C305F/C305F}$ mice did not exhibit noticeable differences in body weight, pathophysiological defects or predisposition to spontaneous tumors from those of the wild type mice.

Mdm2^{C305F} mutation disrupts L5 and L11 binding

To examine the binding activity of the endogenous Mdm2^{C305F} mutant protein, mouse embryonic fibroblasts (MEFs) were isolated at embryonic day 13.5 (E13.5) and an immunoprecipitation-coupled western blot (IP-western) assay was performed. Consistent with previous *in vitro* studies (Lindstrom et al., 2007), Mdm2^{C305F} failed to bind L5 and L11 (Figure 2A). In contrast, Mdm2^{C305F} was able to bind L23 and p53 (Figure 2A-B). The L23-Mdm2 binding can be shown only by IP of L23 but not by IP of Mdm2 due to a potential interference of the anti-Mdm2 antibody (clone 2A10) with L23 binding. To assess E3 ubiquitin ligase activity of Mdm2^{C305F}, we carried out p53 half-life assay using early-passage MEF cells. The half-life of p53 was approximately 30 min under unstressed conditions in both wild type and Mdm2^{C305F} mutant cells (Figure 2C). Likewise, the half-life of Mdm2 itself was found to be also comparable in both wild type and mutant cells, at approximately ten minutes (Figure 2D). Thus, the C305F mutation in the zinc finger does not affect the degradation of p53 or Mdm2 itself. We have noticed that the typical doublet-banding pattern of Mdm2 was somewhat altered by the zinc finger mutation, with the mutant Mdm2^{C305F} showing a stronger top band whereas the wild type Mdm2 showing a stronger bottom band (Figure 2D). The nature of the alteration remains to be clarified.

Mdm2^{C305F} mice retain a normal p53 response to DNA damage

To assess the effect of Mdm2^{C305F} mutation on p53 response to DNA damage, we examined p53 protein levels in MEFs. Early passage MEFs were either left untreated (Control) or treated with 1 μM of Doxorubicin (Dox) or 50J/m^2 of ultraviolet C (UV) light, and p53 was examined by western blotting. As shown in Figure 3A, p53 level was increased to comparable levels among *Mdm2*$^{+/+}$, *Mdm2*$^{+/C305F}$, and *Mdm2*$^{C305F/C305F}$ MEFs after Dox or UV treatment. To ascertain that DNA damage induced p53 transcriptional activity has not been affected, we examined Mdm2 and p21, two archetypal p53 transcriptional targets, in MEFs treated with an increasing amount of Dox. The levels of Mdm2 and p21 increased progressively along with increasing amount of Dox (Figure 3B). Importantly, the levels of Mdm2 and p21 were very comparable between the wild type and the mutant cells at each corresponding Dox dosage.

We next examined p53 response to DNA damage in mouse tissues. Mouse whole-body γ-irradiation causes p53-dependent growth arrest and apoptosis in organs that are sensitive to

radiation, such as intestinal epithelium, spleen, bone marrow, and thymus (Bouvard et al., 2000). Differential responses to irradiation reflect changes of p53 function and can be used as a test for p53 activity *in vivo* (Komarova et al., 2000). We subjected mice to 8-Gy whole-body γ-irradiation, and the stabilization and activation of p53 was assessed in thymus and spleen 18 hours post-treatment. As shown in Figure 3C, the level of p53 was slightly increased after γ-irradiation in both spleen and thymus. The level of p21, on the other hand, was significantly increased, and the increase was similar in organs of the wild type and the *Mdm2*$^{C305F/C305F}$ mice, consistent with results from MEF cells. We have noticed that the basal levels of p53 and p21 in unstressed mutant organs are somewhat elevated, the reason for which has not been determined. We also investigated DNA damage induced apoptosis by TUNEL assay. With γ-irradiation, extensive apoptosis was observed and the levels of apoptosis in organs isolated from wild type and *Mdm2*$^{C305F/C305F}$ mice were essentially identical (Figure 3D). Together, these results support a notion that the p53 DNA damage response is not affected by Mdm2^{C305F} mutation.

Mdm2^{C305F} mutation attenuates p53 response to ribosome biogenesis stress

Given that the Mdm2^{C305F} mutant protein does not interact with L5 and L11 (Figure 2), we sought to determine if a low level Act D induced p53 activation might be attenuated. First, we examined a time-course induction of p53 in MEFs. We observed induction of p53 in the wild type MEFs within 1-2 hours of Act D treatment that was further increased and sustained until termination of the experiment at 12 hours (Figure 4A). In contrast, only a slight induction of p53 at 2- and 4-hour time points was observed *Mdm2*$^{C305F/C305F}$ MEFs (Figure 4A). The intensity of p53 induction correlated with *Mdm2*^{C305F} gene dosage with the wild type cells exhibiting the highest level of p53 induction and the heterozygous cells showing an intermediate induction (Figure 4B). Moreover, we found that a high dose of Act D, 200 nM, elicited equivalent p53 response in MEFs of all genotypes (Figure 4C), consistent with a notion that Act D at this concentration causes DNA double strand breaks (Ljungman et al., 1999), and that *Mdm2*$^{C305F/C305F}$ cells retain a normal p53 response to DNA damage (Figure 3).

Next, we investigated p53 response to Act D in a more physiological setting of mouse skin, which has been extensively used to characterize effects of Act D on cell growth (Bates et al., 1968). The dorsal skins of wild type and *Mdm2*$^{C305F/C305F}$ littermate mice were treated topically with a single dose of 1 μg Act D dissolved in 0.2 ml of acetone, which specifically inhibits ribosomal RNA synthesis with little effect on mRNA or protein synthesis in the mouse skin (Flamm et al., 1966). Negative control mice and 8-Gy γ-irradiated mice were mock treated with 0.2 ml of acetone. 18 hours after the treatment a portion of the skin was formalin fixed and the rest snap-frozen. Western blot analysis of epidermal lysates demonstrated that Act D-induced stabilization of p53 was diminished in *Mdm2*$^{C305F/C305F}$ keratinocytes, whereas the response to γ-irradiation remained intact (Figure 4D).

To determine Act D response on cell proliferation, we carried out cell cycle analysis. We treated early passage wild type and *Mdm2*$^{C305F/C305F}$ MEFs with 5 nM Act D for 18 hours and examined the percentage of cells in S-phase by fluorescence-activated cell sorting (FACS). The FACS analysis showed that the *Mdm2*$^{C305F/C305F}$ cells had a weakened cell

cycle arrest in response to Act D treatment (Figure 4E). Consistent results were obtained from BrdU (5-bromo-2-deoxyuridine) incorporation analysis of Act D treated dorsal mouse skins, inhibition of BrdU incorporation was less pronounced in *Mdm2*$^{C305F/C305F}$ keratinocytes than in wild type keratinocytes (Figure 4F).

We also examined if the Mdm2^{C305F} mutation confers resistance to 5-FU and MPA, two known inhibitors of ribosome biogenesis. We treated MEFs with 5-FU and MPA and determined p53 stabilization by western blotting. Similar to the observations with Act D, p53 induction was attenuated in *Mdm2*$^{C305F/C305F}$ MEFs in a gene dosage dependent manner (Figure 4G). Together, these results indicate that Mdm2 interaction with L5/L11 is important for transducing cellular stress signals that specifically impinge on ribosomal biogenesis, but not DNA damage, to p53.

Myc-induced lymphomagenesis is accelerated by Mdm2^{C305F} mutation

c-Myc up-regulates ribosome biogenesis through direct transactivation of many nucleolar proteins involved in ribosome biogenesis (Ruggero and Pandolfi, 2003). To determine the role of RP-Mdm2-p53 signaling in tumorigenesis, we crossed *Mdm2*$^{C305F/C305F}$ mice with Eμ-*Myc* transgenic mice that constitutively express c-Myc in B-cell lineage and develop B-cell lymphoma at an early age (Adams et al., 1985). Littermates animals (Eμ-*Myc;Mdm2*$^{+/+}$, Eμ-*Myc;Mdm2*$^{+/C305F}$ and Eμ-*Myc;Mdm2*$^{C305F/C305F}$) were monitored daily for signs of morbidity and lymphoma development. Consistent with previous studies, the Eμ-*Myc* transgenic mice with wild type Mdm2 had a median survival time of 20 weeks. The survival of Eμ-*Myc;Mdm2*$^{C305F/C305F}$ compound mice, however, was significantly shortened, showing a median survival of 9 weeks. An intermediate, yet significant, decrease in survival was observed in Eμ-*Myc;Mdm2*$^{+/C305F}$ heterozygous compound mice, showing a median survival of about 15 weeks (Figure 5A). Tumors arising from the Eμ-*Myc;Mdm2*$^{C305F/C305F}$ mice presented with typical lymphadenopathy (Figure 5B), and were phenotypically indistinguishable from those occurring in Eμ-*Myc;Mdm2*$^{+/+}$ mice. These results suggest that the RP-Mdm2-p53 signaling, in addition to p19Arf-Mdm2-p53 signaling, may be another stress response barrier against Myc-induced lymphomagenesis.

To determine the mechanism leading to accelerated lymphomagenesis in the Eμ-*Myc;Mdm2*$^{C305F/C305F}$ compound mice, we isolated spleen and thymus tissues from tumor-bearing Eμ-*Myc;Mdm2*$^{+/+}$, Eμ-*Myc;Mdm2*$^{+/C305F}$ and Eμ-*Myc;Mdm2*$^{C305F/C305F}$ animals, as well as from age-matched non-transgenic wild type mice, and determined protein levels of L5 and L11. In agreement with recent studies showing c-Myc driving overexpression of ribosomal proteins (Boon et al., 2001; Coller et al., 2000; Menssen and Hermeking, 2002), we found that the levels of L5 and L11 were highly elevated in tissues expressing Eμ-*Myc*, and the elevation is irrespective of the Mdm2 C305F mutation (Figure 5C). We also observed similar up-regulation (Zhu et al., 2009)of several other ribosomal proteins including L23, L26, S9, and S6 (data not shown). We noticed that the Actin level appears to be lower in organs expressing Eμ-*Myc* when lysates containing equal amount of total protein were analyzed using immunoblotting. Therefore, in this case, Actin-based loading control would only underestimate the extent of L5/L11 overexpression. Prior study demonstrates that inhibition of ribosome biogenesis induces translocation of L11 from nucleolus to

nucleoplasm (Bhat et al., 2004), we therefore investigated if c-Myc induced L5 and L11 overexpression could result in their nucleoplasmic accumulation, where they are in proximity with and can bind to Mdm2. We isolated spleens from 4-week old non-tumor bearing animals. At this age the spleens from Eμ-*Myc* transgenics are moderately hyperplastic, but still comparable to wild type spleens in terms of organ size and morphology. We fractionated splenocyte lysates into total (TO), cytoplasmic (Cyto), nucleoplasmic (NP), and nucleolar (NO) fractions and examined L11 protein levels. Splenocytes isolated from tumor-free, young Eμ-*Myc* transgenics expressed a higher level of total L11 than do the non-transgenics (Figure 5D, compare lanes 1-2). Importantly, L11 was more prominent in the NP fraction of Eμ-*Myc* transgenic splenocytes than of non-transgenic splenocytes (Figure 5D, compare lanes 5-6). To further determine the consequence of increased L11 in the nucleoplasm, we carried out anti-Mdm2 IP-western assay with spleens isolated from non-tumor-bearing Eμ-*Myc;Mdm2*$^{C305F/C305F}$ mice and from control Eμ-*Myc;Mdm2*$^{+/+}$ littermates. As expected, Mdm2 interacted with L11 in lysates isolated from the Eμ-*Myc;Mdm2*$^{+/+}$ splenocytes; whereas the L11 in Eμ-*Myc;Mdm2*$^{C305F/C305F}$ splenocytes, even though expressed to a higher level than in Eμ-*Myc;Mdm2*$^{+/+}$ splenocytes, showed very little interactions with Mdm2 (Figure 5E). Collectively, these data demonstrate that loss of L11-Mdm2 interaction due to the Mdm2 zinc finger C305F mutation accelerated oncogenic c-Myc-induced lymphomagenesis. The data also show that in c-Myc overexpressing cells L11 is highly expressed and enriched in the nucleus where it can interact with Mdm2, but not with Mdm2^{C305F}. Altogether, this suggests that disabling the L11-Mdm2 interaction can compromise, at least in part, p53 response to oncogenic c-Myc.

p19Arf is not required for p53 response to ribosomal stress

We have noticed that the median survival of Eμ-*Myc;Mdm2*$^{C305F/C305F}$ mice (9 weeks, Figure 5A) is very similar to that of Eμ-*Myc;p19Arf*$^{-/-}$ mice (8-weeks) (Eischen et al., 1999). We speculated that the p53 signaling mediated by RP-Mdm2 interaction and by p19Arf-Mdm2 interaction are parallel pathways both required for anti Myc induced tumorigenesis, elimination of either one results in accelerated tumor formation. Alternatively, the two pathways may function in a linear fashion, and mutations in Mdm2 that disrupt RP binding also affect p19Arf function. To gain insight into possible interlink between the two pathways, we first determined if p19Arf mediated oncogenic signaling is compromised by the Mdm2 mutation. To reduce individual variations duplicate mice were used in each sample group. We isolated splenic extracts from 4 week-old non-tumor bearing Eμ-*Myc;Mdm2*$^{+/+}$ and Eμ-*Myc;Mdm2*$^{C305F/C305F}$ transgenics, as well as from their non-transgenic counterparts. The extracts were immunoblotted for L11, p19Arf and p53. In line with a previous study (Eischen et al., 1999), Eμ-*Myc* expression resulted in elevated p19Arf expression in splenic B cells (Figure 6A, lanes 5-6). Elevated p19Arf expression was also observed in transgenic Mdm2^{C305F} mutant mice (Figure 6A, lanes 7-8), indicating that c-Myc mediated induction of p19Arf does not required L11-Mdm2 binding. Importantly, we observed evident p53 induction in spleens of Eμ-*Myc;Mdm2*$^{+/+}$ transgenics, but less so in spleens of Eμ-*Myc;Mdm2*$^{C305F/C305F}$ mice. This is consistent with a notion that the RP-Mdm2-p53 pathway is important in oncogenic c-Myc induction of p53.

While sustained c-Myc expression elicits a p19Arf mediated p53 response, additional p19Arf independent mechanisms of c-Myc induction of p53 exist (Zindy et al., 1998). Consistently, we found that both *Mdm2*$^{C305F/C305F}$ and *p19Arf*$^{-/-}$ MEFs transiently expressing c-Myc had comparable elevated p53 levels, but was lower than that of wild type MEFs (Figure 6B), suggesting that the RP-Mdm2-p53 and the p19Arf-Mdm2-p53 pathways act independently and are each contributing to c-Myc induction of p53. To further ascertain that the ribosomal stress induced p53 is through a p19Arf independent mechanism, we investigated p53 induction in *p19Arf*$^{-/-}$ MEF cells treated with Act D. Western blotting demonstrated that in both wild type and *p19Arf*$^{-/-}$ MEF cells p53 is induced similarly by a low level of Act D at comparable kinetics (Figure 6C). Furthermore, we noticed that Mdm2, a p53 target, was also induced with similar kinetics. Similar results were also obtained by treating cells with MPA (Figure 6D). Hence, the data indicate that p19Arf is not required for ribosomal inhibition induced p53 activation. Finally, we examined Mdm2-p19Arf interaction in Act D treated Mdm2^{C305F} mutant MEFs. Act D treatment resulted in high-level expression of p53 and Mdm2 in wild type but not Mdm2^{C305F} MEFs; the treatment also resulted in high-level expression of p53 and Mdm2 in p19Arf-null MEFs (Figure 6E, Loading). Immunoprecipitation demonstrated that Mdm2^{C305F} mutant protein interacts effectively with p19Arf, but not with L11 (Figure 6E, Lanes 3-4). Additionally, wild type Mdm2 interacted with L11 in p19Arf-null MEFs and the interaction was enhanced upon Act D treatment (Figure 6E, Lanes 5-6). It is worth mentioning that the basal levels of p19Arf expression are slightly lower in Mdm2^{C305F} MEFs than in wild type MEFs. Whether this is a variation of MEF cell clones or is directly related to Mdm2^{C305F} mutation remains to be determined.

Discussion

A number of ribosomal proteins, including L5, L11, L23, L26, S3 and S7, have been shown to interact with and inhibit the E3 ligase function of Mdm2, thereby stabilizing and activating p53 (Chen et al., 2007; Dai and Lu, 2004; Dai et al., 2004; Jin et al., 2004; Lohrum et al., 2003; Ofir-Rosenfeld et al., 2008; Zhang et al., 2003; Zhu et al., 2009). The physiological significance of the RP-Mdm2 interaction, however, has not been previously studied *in vivo*. In this study, we generated and analyzed mice carrying a C305F knockin mutation in the *Mdm2* zinc finger. The mutation disrupts the interaction of Mdm2 with L5 and L11. Several important observations have been made from this study.

An RP-Mdm2-p53 signaling pathway sensing inhibition of ribosome biogenesis

The generation of *Mdm2*^{C305F} mutant mice has allowed for a detailed *in vivo* characterization for the role of RP-Mdm2 binding in p53 response to ribosome biogenesis perturbations. Our data show that upon DNA damage, the response of the mutant mice is indistinguishable from that of wild type animals in terms of p53 activation, cell cycle arrest, and apoptosis. These data indicate that the integrity of the Mdm2 zinc finger and thus the binding of L5 and L11 are not required for p53 DNA damage response. In contrast, p53 response to treating animals with inhibitors that cause specifically inhibition of ribosomal biogenesis or nucleolar stress, but not DNA damage, is significantly compromised in mutant animals. The failure of *Mdm2*^{C305F} animals to respond to nucleolar stress is in agreement

with previous *in vitro* studies, where knockdown of L11 results in an attenuated p53 response to the same forms of inhibitions (Bhat et al., 2004; Lohrum et al., 2003; Zhang et al., 2003). It also corroborates our recent report that ectopically expressed $Mdm2^{C305F}$ does not interact with L11, and that p53 activity that has been suppressed by ectopically expressed $Mdm2^{C305F}$ cannot be restored by L11 overexpression (Lindstrom et al., 2007). Also consistent with *in vitro* data, we have found that $Mdm2^{C305F}$ retains ability to interact with L23 and p53 as well as with p19Arf. It seems that Mdm2 binding to L23, without binding to L5 and L11, is insufficient for p53's response to ribosomal stress. A recent study has shown that L11 cooperates with L5 to inhibit Mdm2. When co-expressed the inhibitory activity of L5 and L11 towards Mdm2 is enhanced (Horn and Vousden, 2008). It remains to be studied if such a relationship exists in the context of L23. Nonetheless, the bulk of studies and available genetic models tend to favor L11 as the prime mediator of p53 ribosomal stress response via inhibition of Mdm2 (see below).

At the concentrations used in our study (5 nM), Act D specifically inhibits RNA pol I-dependent transcription (Iapalucci-Espinoza and Franze-Fernandez, 1979; Perry and Kelley, 1970) causing nucleolar stress, without causing DNA damage. Consistently, genetic ablation of RNA Pol I transcription initiation factor TIF-IA, which abrogates Pol I transcription, elicits a p53 response (Yuan et al., 2005). In this sense, low dose Act D treatment is akin to genetic ablation of TIF-IA. In fact, as is in the case with Act D treatment, ablation of TIF-IA in MEFs evokes breakdown of the nucleolus, elicits the binding of L11 to Mdm2 and results in p53 activation (Yuan et al., 2005). The Belly Spot and Tail (Bst) mice, which have a point mutation in the ribosomal protein gene *RPL24*, provide yet another genetic evidence for the existence of an RP-Mdm2-p53 signaling pathway. Mice heterozygous for *RPL24* ($Bst^{+/-}$ mice) have impaired ribosomal biogenesis leading to various congenital abnormalities (Oliver et al., 2004). Interestingly, impairment of ribosome biogenesis in the $Bst^{+/-}$ mice elicits a p53 response that is also mediated by L11 inhibition of Mdm2 (Barkic et al., 2009). In conjunction with the work presented herein, accumulating evidences from both *in vitro* and *in vivo* studies point to existence of a *bona fide* p53 responsive ribosomal biogenesis stress checkpoint (Figure 7A).

The L5/L11-Mdm2-p53 signaling pathway is required for preventing oncogenic c-Myc induced tumorigenesis

The proto-oncogene product c-Myc has been shown to directly regulate ribosome biogenesis through the transcription of genes encoding nucleolar proteins involved in ribosome biogenesis as well as some ribosomal proteins (Ruggero and Pandolfi, 2003). However, it remains unknown whether c-Myc-driven ribosome biogenesis is directly responsible for tumor promotion. We postulated that the L11-Mdm2 interaction constitutes a checkpoint for superfluous production of ribosomal proteins resulting from oncogenic overexpression of c-Myc. To test this hypothesis, we generated and analyzed Eμ-*Myc;*$Mdm2^{C305F/C305F}$ mice. Eμ-*myc* transgenic mice develop B-cell lymphomas (Adams et al., 1985), similar to those observed in human Burkitt's lymphomas bearing a translocated (t8;14) c-*MYC* allele (Alitalo et al., 1987). Strikingly, we show that lymphomagenesis of Eμ-*Myc* mice is greatly accelerated in the presence of $Mdm2^{C305F}$. Mechanistically, c-Myc induces overexpression of L11, which accumulates in the nucleus and binds to Mdm2 but not $Mdm2^{C305F}$. The

accelerated morbidity imparted by the Mdm2^{C305F} mutation is thus likely due to the loss of L11 binding to Mdm2^{C305F}. In regards to L23, it is clear that retention of L23 binding to Mdm2^{C305F} is insufficient to compensate for loss of L11 or L5 binding in deterring c-Myc lymphomagenesis in the Eμ-*Myc;Mdm2*$^{C305F/C305F}$ mice. Moreover, although the genes encoding for L11 and L23 are c-Myc target genes, L11 is involved in a negative feedback loop with c-Myc, while L23 actually enables c-Myc to promote cell cycle progression (Dai et al., 2007; Wanzel et al., 2008). Collectively, these results indicate that the L11-Mdm2-p53 signaling plays an indispensable role in deterring c-Myc mediated tumorigenesis.

p19Arf-Mdm2-p53 and L11-Mdm2-p53 are parallel signaling pathways

Our results raise an interesting question with regard to cooperation between the p19Arf-Mdm2-p53 and the L11-Mdm2-p53 pathways. It is conceivable that p19Arf can impact ribosomal biogenesis through inhibiting the processing of pre-ribosomal RNA (Sugimoto et al., 2003), at least in part, through its interaction with and inhibiting the function of B23 (NPM) (Itahana et al., 2003), an endoribonuclease essential for pre-rRNA processing (Herrera et al., 1995; Savkur and Olson, 1998). Consequently, such a p19Arf function can cause perturbation of ribosomal biogenesis and activate the L11-Mdm2-p53 pathway. However, while p19Arf can cause ribosome biogenesis stress *per se*, it is dispensable for the induction of p53 resulting from such stress, as demonstrated by the unaltered p53 response and L11-Mdm2 binding upon nucleolar stress in *p19Arf*$^{-/-}$ MEFs. In addition, even though *Mdm2*$^{C305F/C305F}$ MEFs lack p53 response to Act D treatment, the binding of Mdm2^{C305F} mutant protein to p19Arf remains intact.

Oncogenic c-Myc can induce p53 through p19Arf independent pathways (Zindy et al., 1998). In support, c-Myc expression elicited ample p53 response in p19Arf-null MEF cells (Figure 6B). Given the role of c-Myc in promoting ribosomal biogenesis, this p19Arf independent induction of p53 by c-Myc may very well be ribosomal protein mediated. This notion suggests that p53 can safeguard against c-Myc tumorigenesis via two independent signaling pathways, a p19Arf-Mdm2-p53 pathway and a ribosomal protein-Mdm2-p53 pathway (Figure 7B). Accordingly, disruption of either one will accelerate c-Myc induced tumor formation. This was illustrated by remarkably similar short survival time of Eμ-*Myc;Mdm2*$^{C305F/C305F}$ mice and Eμ-*Myc;p19Arf*$^{-/-}$ mice. Given the data showing similar susceptibility of Eμ-*Myc;Mdm2*$^{C305F/C305F}$ and Eμ-*Myc;p19Arf*$^{-/-}$ transgenic animals to tumor development, one prediction will be that an even shorter latency of Myc-driven tumor formation might be found in compound mice carrying both *Mdm2*$^{C305F/C305F}$ mutation and *p19Arf* deletion. In conclusion, our data support a model that the p19Arf-Mdm2-p53 and the RP-Mdm2-p53 pathways are independent, parallel pathways working together to protect cells from oncogenic c-Myc induced tumorigenesis (Figure 7B).

The Mdm2^{C305F} knockin mouse model provides evidence for a prevailing *in vivo* checkpoint, mediated by L11-Mdm2 interaction, to monitor the integrity of ribosome biogenesis and activate p53 when this process goes awry. The L11-Mdm2-p53 signaling pathway is not required for DNA damage induction of p53, in that the mutant mice respond to DNA damage and induce p53 activity as efficiently as their wild type counterparts. Moreover, our data establish the L11-Mdm2-p53 pathway as an important *in vivo* barrier for

defending against oncogenic c-Myc induced tumorigenesis, parallel to the p19Arf-Mdm2-p53 signaling. p19Arf, through interaction with Mdm2, mediates a p53-dependent checkpoint in response to a broad range of oncogenic insults, including elevated expression of Myc, E2F1, Ras, E1A, and v-Abl (Sherr, 1998). In this sense, it is conceivable that L11-Mdm2-p53 signaling also mediates a p53-dependent checkpoint in response to deregulated oncogenes that promote superfluous ribosome biogenesis. For instance, E2F1 specifically interacts with and enhances rRNA promoter activity through two E2F1-binding sequences (Ayrault et al., 2006); oncogenic Ras influences mTOR activity and thus protein translation through modulating the PI3K-Akt signaling cascade (Fingar and Blenis, 2004). In both cases the oncogenic activity of E2F1 and Ras promotes ribosomal biogenesis either directly or indirectly. Whether the L11-Mdm2-p53 signaling is a general oncogenic surveillance signaling that responses to a broad range of deregulated oncogenes including E2F1 and Ras or is only specific to c-Myc remains to be determined.

Materials and Methods

Generation of Mdm2^{C305F} knockin mice

Murine 129/Sv genomic DNA containing the last six exons (exons 7–12) of Mdm2 was a gift from Dr. Lozano (University of Texas, M.D. Anderson Cancer Center). The targeting vector was constructed in a PGK neo vector backbone. A cysteine to phenylalanine substitution was introduced in codon 305 (C305F) using site-directed mutagenesis (TGT>TTT). A new *Spe1* restriction site (ACT AGT) was generated at the same time (TGT ACC TCA > TTT *ACT AGT*). DNA isolated from G418-resistant ES cell colonies was subjected to *BamH1* digestion followed by Southern blot analysis using a probe covering intron 9 between exons 9 and 10. The presence of the C305F substitution was further confirmed by PCR amplification of genomic DNA using primers flanking exon 12, followed by *Spe1* digestion. One positive clone was injected into blastocysts, and transferred into pseudopregnant female recipients. Germline transmission was confirmed by Southern blot and PCR analysis. *Neomycin* selection marker was deleted by crossing germline transmitted *Mdm2*$^{+/C305F}$ mice with Ella-*Cre* transgenic mice (Jackson Laboratories, stock number 003724). The resulting males were mated with C57BL/6 females and backcrossed to C57BL/6 for 5 generations.

Mouse experiments

Mice were bred and maintained strictly under protocol (#07-056) approved by the Institutional Animal Care and Use Committee in the UNC Animal Care Facility. For BrdU incorporation experiment, mice were injected intraperitoneally with BrdU (50 mg/gram body weight) 30 minutes prior to euthanasia. BrdU incorporation was detected by immunohistochemical staining of paraffin-embedded tissue sections with mouse anti-BrdU (Ab-2) monoclonal antibody (Calbiochem, San Diego, CA, USA), biotin-conjugated anti-mouse antibody (Vector Laboratories, Inc., Burlingame, CA, USA) and an avidin–biotin–peroxidase kit (Vectastain Elite, Vector Laboratories, Inc.) with diaminobenzidine as a chromogen. The percentage of BrdU positive cells from the total number of interfollicular keratinocytes in 200 μm fields and 15 fields per mouse were quantified. For mouse skin treatments, mice from each genotype were shaven 24 hours prior to treatment. The dorsal

skin was treated topically for 18 hours with a single dose of Act D at 1 ug/200ul in acetone or acetone only. For apoptosis studies, TUNEL assay was carried out using an ApopTag® Peroxidase *In Situ* Apoptosis Detection Kit *(*Calbiochem #S7100). For c-Myc mediated tumorigenesis study, $Mdm2^{C305F/C305F}$ females were bred with Eμ-*Myc* transgenic males to obtain Eμ-$Myc;Mdm2^{+/C305F}$ offspring, which were then crossed with $Mdm2^{C305F/C305F}$ mice to obtain Eμ-$Myc;Mdm2^{C305F/C305F}$ compound mice. Eμ-*Myc* mice were purchased from The Jackson Laboratory (stock number 002728). For survival study, mice were palpated regularly for early signs of inguinal lymph node enlargement and monitored for tumor progression and signs of morbidity. Moribund mice were humanely euthanized by CO_2 asphyxiation followed by a second method to ensure euthanasia. Mouse tumors and organs were fixed in formalin for histopathology and snap frozen for protein and RNA extraction.

Cell Culture

Primary mouse embryo fibroblasts (MEF) were isolated on embryonic (E) day 13.5 and grown in a 37°C incubator with 5% CO_2 in DMEM supplied with 10% FBS and penicillin-streptomycin. MEF cells were treated as indicated with 5 nM or 200 nM actinomycin D (Act D), 2 μM mycophenolic acid (MPA), 1 μM doxorubicin (Dox) or 10 μM 5-fluorouracil (5-FU). For retrovirus infections, $Mdm2^{+/+}$, $Mdm2^{C305F/C305F}$ and $p19Arf^{-/-}$ MEF cells were infected with retroviruses expressing c-Myc or pBabe control vector and selected with puromycin (2.5 ug/ml) for 3 days. Retrovirus infected MEFs were then allowed to recover for 48 hours and harvested for analysis.

Protein Analysis

For western blot, MEF cells were lysed with 0.5% NP-40 lysis buffer for straight westerns or 0.1% NP-40 lysis buffer for co-immunoprecipitation experiments. For mouse tissue protein extraction, spleens, thymus and lymphoma tissues were ground by pestle and mortar with liquid N_2 and the protein was extracted with 0.5% NP-40 lysis buffer. For protein analysis of epidermal keratinocytes, the epidermal skin layer was scraped off excised skin using a razorblade and extracted with 0.5% NP-40 lysis buffer. To assess the half-life of p53 and Mdm2, low passage MEF cells were treated with cycloheximide (50 ug/ml), chased for the indicated time points and harvested with SDS lysis buffer (2% SDS, 10% glycerol, 50 mM Tris). Mouse monoclonal anti Mdm2 (2A10 and 4B11, Calbiochem), p53 (NCL-505, Novocastra; DO-1, Lab Vision/Neomarkers), actin (MAB1501, Chemicon International), goat polyclonal anti p53 (FL-393; Santa Cruz), and rat polyclonal anti p19Arf (Santa Cruz) antibodies were purchased commercially. Rabbit polyclonal antibodies to p21 were gifts from Dr. Yue Xiong (UNC-Chapel Hill). Rabbit polyclonal antibodies to L5 and L11 were made in house and previously described (Lindstrom et al., 2007).

Cellular Fractionation

Protocol for nucleolar fractionation was adapted from a previously described method by Muramatsu and coworkers (Muramatsu et al., 1974). Freshly harvested mouse spleens were mechanically disassociated between two glass microscope slides. Large debris was allowed to settle and single cell suspension was centrifuged at 200*g* for 10 min and washed 2X with

RPMI (Roswell Park Memorial Institute) medium. Red blood cell lysis was carried out using NH_4Cl lysis buffer (0.75% NH_4Cl, 0.017 M Tris-HCl, pH 7.2) for 5 min at room temperature. Splenocytes were resuspended in 1 ml of RSB buffer (10 mM Hepes, pH 7.9, 10 mM KCl, 1.5 mM MgCl2, 0.5 mM DTT) and placed on ice for 10 min. Cell membranes were then broken using a Dounce homogenizer (tight pestle A). Nuclei (pellet) were collected by centrifugation at 218*g* for 5 min and resuspended in 3 ml of 0.25 M sucrose/10 mM $MgCl_2$ and overlaid onto 3 ml of 0.88 M sucrose/0.05 mM $MgCl_2$ and purified by centrifugation at 1430*g* for 10 min. The pelleted nuclei were resuspended in 2 ml of 0.34 M sucrose/0.05 mM $MgCl_2$ and sonicated for 60 seconds with 10 seconds intervals. The sonicated cell lysate was then overlaid onto 3 ml of 0.88 M sucrose/0.05 mM $MgCl_2$ and centrifuged at 3000*g* for 10 min. The pellet contained the purified nucleoli and the supernatant represented the nucleoplasmic fraction. Protease inhibitor cocktail was added freshly to all buffers before use.

Statistical analysis

Statistical analysis was performed using GraphPad Prism 4 Software (GraphPad Software, San Diego, CA, USA). For Eμ-Myc tumorigenesis experiments a Kaplan-Meier survival curve was performed. A one-way analysis of variance test with Tukey's multiple comparison post test was performed for BrdU incorporation experiments.

Acknowledgements

We thank Koji Itahana, Yoko Itahana and Kim Gooding for their helpful advice and technical assistance. Y.Z. is a recipient of a Career Award in Biomedical Science from the Burroughs Wellcome Fund, Howard Temin Award from the National Cancer Institute, and Scholar Award from the Leukemia & Lymphoma Society. This study was supported by grants from the NIH and the American Cancer Society to Y.Z.

References

Adams JM, Harris AW, Pinkert CA, Corcoran LM, Alexander WS, Cory S, Palmiter RD, Brinster RL. The c-myc oncogene driven by immunoglobulin enhancers induces lymphoid malignancy in transgenic mice. Nature. 1985; 318:533–538. [PubMed: 3906410]

Alitalo K, Koskinen P, Makela TP, Saksela K, Sistonen L, Winqvist R. myc oncogenes: activation and amplification. Biochim Biophys Acta. 1987; 907:1–32. [PubMed: 3552050]

Allison AC. Mechanisms of action of mycophenolate mofetil. Lupus. 2005; 14(Suppl 1):s2–8. [PubMed: 15803924]

Ayrault O, Andrique L, Seite P. Involvement of the transcriptional factor E2F1 in the regulation of the rRNA promoter. Exp Cell Res. 2006; 312:1185–1193. [PubMed: 16510138]

Barkic M, Crnomarkovic S, Grabusic K, Bogetic I, Panic L, Tamarut S, Cokaric M, Jeric I, Vidak S, Volarevic S. The p53 tumor suppressor causes congenital malformations in Rpl24-deficient mice and promotes their survival. Mol Cell Biol. 2009; 29:2489–2504. [PubMed: 19273598]

Bates RR, Wortham JS, Counts WB, Dingman CW, Gelboin HV. Inhibition by actinomycin D of DNA synthesis and skin tumorigenesis induced by 7,12-dimethylbenz(a)anthracene. Cancer Res. 1968; 28:27–34. [PubMed: 5635369]

Bhat KP, Itahana K, Jin A, Zhang Y. Essential role of ribosomal protein L11 in mediating growth inhibition-induced p53 activation. Embo J. 2004; 23:2402–2412. [PubMed: 15152193]

Boon K, Caron HN, van Asperen R, Valentijn L, Hermus MC, van Sluis P, Roobeek I, Weis I, Voute PA, Schwab M, Versteeg R. N-myc enhances the expression of a large set of genes functioning in ribosome biogenesis and protein synthesis. EMBO J. 2001; 20:1383–1393. [PubMed: 11250904]

Bouvard V, Zaitchouk T, Vacher M, Duthu A, Canivet M, Choisy-Rossi C, Nieruchalski M, May E. Tissue and cell-specific expression of the p53-target genes: bax, fas, mdm2 and waf1/p21, before and following ionising irradiation in mice. Oncogene. 2000; 19:649–660. [PubMed: 10698510]

Chen D, Zhang Z, Li M, Wang W, Li Y, Rayburn ER, Hill DL, Wang H, Zhang R. Ribosomal protein S7 as a novel modulator of p53-MDM2 interaction: binding to MDM2, stabilization of p53 protein, and activation of p53 function. Oncogene. 2007

Coller HA, Grandori C, Tamayo P, Colbert T, Lander ES, Eisenman RN, Golub TR. Expression analysis with oligonucleotide microarrays reveals that MYC regulates genes involved in growth, cell cycle, signaling, and adhesion. Proc Natl Acad Sci U S A. 2000; 97:3260–3265. [PubMed: 10737792]

Corvi R, Savelyeva L, Amler L, Handgretinger R, Schwab M. Cytogenetic evolution of MYCN and MDM2 amplification in the neuroblastoma LS tumour and its cell line. Eur J Cancer. 1995; 31A: 520–523. [PubMed: 7576957]

Dai MS, Arnold H, Sun XX, Sears R, Lu H. Inhibition of c-Myc activity by ribosomal protein L11. EMBO J. 2007; 26:3332–3345. [PubMed: 17599065]

Dai MS, Jin Y, Gallegos JR, Lu H. Balance of Yin and Yang: ubiquitylation-mediated regulation of p53 and c-Myc. Neoplasia. 2006; 8:630–644. [PubMed: 16925946]

Dai MS, Lu H. Inhibition of MDM2-mediated p53 ubiquitination and degradation by ribosomal protein L5. J Biol Chem. 2004; 279:44475–44482. [PubMed: 15308643]

Dai MS, Sun XX, Lu H. Aberrant expression of nucleostemin activates p53 and induces cell cycle arrest via inhibition of MDM2. Mol Cell Biol. 2008; 28:4365–4376. [PubMed: 18426907]

Dai MS, Zeng SX, Jin Y, Sun XX, David L, Lu H. Ribosomal protein L23 activates p53 by inhibiting MDM2 function in response to ribosomal perturbation but not to translation inhibition. Mol Cell Biol. 2004; 24:7654–7668. [PubMed: 15314173]

Eischen CM, Weber JD, Roussel MF, Sherr CJ, Cleveland JL. Disruption of the ARF-MDM2-p53 tumor suppressor pathway in Myc-induced lymphomagenesis. Genes & Dev. 1999; 13:2658–2669. [PubMed: 10541552]

Fingar DC, Blenis J. Target of rapamycin (TOR): an integrator of nutrient and growth factor signals and coordinator of cell growth and cell cycle progression. Oncogene. 2004; 23:3151–3171. [PubMed: 15094765]

Flamm WG, Banerjee MR, Counts WB. Topical application of actinomycin D on mouse skin: effect on the synthesis of ribonucleic acid and protein. Cancer Res. 1966; 26:1349–1360. [PubMed: 5911575]

Fumagalli S, Di Cara A, Neb-Gulati A, Natt F, Schwemberger S, Hall J, Babcock GF, Bernardi R, Pandolfi PP, Thomas G. Absence of nucleolar disruption after impairment of 40S ribosome biogenesis reveals an rpL11-translation-dependent mechanism of p53 induction. Nat Cell Biol. 2009; 11:501–508. [PubMed: 19287375]

Gilkes DM, Chen L, Chen J. MDMX regulation of p53 response to ribosomal stress. Embo J. 2006; 25:5614–5625. [PubMed: 17110929]

Herrera JE, Savkur R, Olson MO. The ribonuclease activity of nucleolar protein B23. Nucleic Acids Res. 1995; 23:3974–3979. [PubMed: 7479045]

Horn HF, Vousden KH. Cooperation between the ribosomal proteins L5 and L11 in the p53 pathway. Oncogene. 2008; 27:5774–5784. [PubMed: 18560357]

Iapalucci-Espinoza S, Franze-Fernandez MT. Effect of protein synthesis inhibitors and low concentrations of actinomycin D on ribosomal RNA synthesis. FEBS Lett. 1979; 107:281–284. [PubMed: 510537]

Itahana K, Bhat KP, Jin A, Itahana Y, Hawke D, Kobayashi R, Zhang Y. Tumor suppressor ARF degrades B23, a nucleolar protein Involved in ribosome biogenesis and cell proliferation. Mol Cell. 2003; 12:1151–1164. [PubMed: 14636574]

Jin A, Itahana K, O'Keefe K, Zhang Y. Inhibition of HDM2 and activation of p53 by ribosomal protein L23. Mol Cell Biol. 2004; 24:7669–7680. [PubMed: 15314174]

Komarova EA, Christov K, Faerman AI, Gudkov AV. Different impact of p53 and p21 on the radiation response of mouse tissues. Oncogene. 2000; 19:3791–3798. [PubMed: 10949934]

Lindstrom MS, Jin A, Deisenroth C, White Wolf G, Zhang Y. Cancer-Associated Mutations in the MDM2 Zinc Finger Domain Disrupt Ribosomal Protein Interaction and Attenuate MDM2-Induced p53 Degradation. Mol Cell Biol. 2007; 27:1056–1068. [PubMed: 17116689]

Ljungman M, Zhang F, Chen F, Rainbow AJ, McKay BC. Inhibition of RNA polymerase II as a trigger for the p53 response. Oncogene. 1999; 18:583–592. [PubMed: 9989808]

Lohrum MA, Ludwig RL, Kubbutat MH, Hanlon M, Vousden KH. Regulation of HDM2 activity by the ribosomal protein L11. Cancer Cell. 2003; 3:577–587. [PubMed: 12842086]

Longley DB, Harkin DP, Johnston PG. 5-fluorouracil: mechanisms of action and clinical strategies. Nat Rev Cancer. 2003; 3:330–338. [PubMed: 12724731]

Menssen A, Hermeking H. Characterization of the c-MYC-regulated transcriptome by SAGE: identification and analysis of c-MYC target genes. Proc Natl Acad Sci U S A. 2002; 99:6274–6279. [PubMed: 11983916]

Muramatsu M, Hayashi Y, Onishi T, Sakai M, Takai K. Rapid isolation of nucleoli from detergent purified nuclei of various tumor and tissue culture cells. Exp Cell Res. 1974; 88:245–251. [PubMed: 4372069]

Ofir-Rosenfeld Y, Boggs K, Michael D, Kastan MB, Oren M. Mdm2 regulates p53 mRNA translation through inhibitory interactions with ribosomal protein L26. Mol Cell. 2008; 32:180–189. [PubMed: 18951086]

Oliner JD, Kinzler KW, Meltzer PS, George DL, Vogelstein B. Amplification of a gene encoding a p53-associated protein in human sarcomas. Nature. 1992; 358:80–83. [PubMed: 1614537]

Oliver ER, Saunders TL, Tarle SA, Glaser T. Ribosomal protein L24 defect in belly spot and tail (Bst), a mouse Minute. Development. 2004; 131:3907–3920. [PubMed: 15289434]

Perry RP. Balanced production of ribosomal proteins. Gene. 2007; 401:1–3. [PubMed: 17689889]

Perry RP, Kelley DE. Inhibition of RNA synthesis by actinomycin D: characteristic dose-response of different RNA species. J Cell Physiol. 1970; 76:127–139. [PubMed: 5500970]

Picksley SM, Lane DP. The p53-mdm2 autoregulatory feedback loop: a paradigm for the regulation of growth control by p53? Bioessays. 1993; 15:689–690. [PubMed: 7506024]

Reifenberger G, Liu L, Ichimura K, Schmidt EE, Collins VP. Amplification and overexpression of the MDM2 gene in a subset of human malignant gliomas without p53 mutations. Cancer Res. 1993; 53:2736–2739. [PubMed: 8504413]

Rubbi CP, Milner J. Disruption of the nucleolus mediates stabilization of p53 in response to DNA damage and other stresses. Embo J. 2003; 22:6068–6077. [PubMed: 14609953]

Ruggero D, Pandolfi PP. Does the ribosome translate cancer? Nat Rev Cancer. 2003; 3:179–192. [PubMed: 12612653]

Savkur RS, Olson MO. Preferential cleavage in pre-ribosomal RNA byprotein B23 endoribonuclease. Nucleic Acids Res. 1998; 26:4508–4515. [PubMed: 9742256]

Schlott T, Reimer S, Jahns A, Ohlenbusch A, Ruschenburg I, Nagel H, Droese M. Point mutations and nucleotide insertions in the MDM2 zinc finger structure of human tumors. JPathol. 1997; 182:54–61. [PubMed: 9227342]

Sherr CJ. Tumor surveillance via the ARF-p53 pathway. Genes & Dev. 1998; 12:2984–2991. [PubMed: 9765200]

Sugimoto M, Kuo ML, Roussel MF, Sherr CJ. Nucleolar Arf tumor suppressor inhibits ribosomal RNA processing. Mol Cell. 2003; 11:415–424. [PubMed: 12620229]

Sun XX, Dai MS, Lu H. 5-fluorouracil activation of p53 involves an MDM2-ribosomal protein interaction. J Biol Chem. 2007; 282:8052–8059. [PubMed: 17242401]

Sun XX, Dai MS, Lu H. Mycophenolic acid activation of p53 requires ribosomal proteins L5 and L11. J Biol Chem. 2008; 283:12387–12392. [PubMed: 18305114]

Tamborini E, Della Torre G, Lavarino C, Azzarelli A, Carpinelli P, Pierotti MA, Pilotti S. Analysis of the molecular species generated by MDM2 gene amplification in liposarcomas. Int J Cancer. 2001; 92:790–796. [PubMed: 11351297]

Vogelstein B, Lane D, Levine AJ. Surfing the p53 network. Nature. 2000; 408:307–310. [PubMed: 11099028]

Wanzel M, Russ AC, Kleine-Kohlbrecher D, Colombo E, Pelicci PG, Eilers M. A ribosomal protein L23-nucleophosmin circuit coordinates Mizl function with cell growth. Nat Cell Biol. 2008; 10:1051–1061. [PubMed: 19160485]

Yuan X, Zhou Y, Casanova E, Chai M, Kiss E, Grone HJ, Schutz G, Grummt I. Genetic inactivation of the transcription factor TIF-IA leads to nucleolar disruption, cell cycle arrest, and p53-mediated apoptosis. Mol Cell. 2005; 19:77–87. [PubMed: 15989966]

Zhang Y, Lu H. Signaling to p53: ribosomal proteins find their way. Cancer Cell. 2009; 16:369–377. [PubMed: 19878869]

Zhang Y, Wolf GW, Bhat K, Jin A, Allio T, Burkhart WA, Xiong Y. Ribosomal protein L11 negatively regulates oncoprotein MDM2 and mediates a p53-dependent ribosomal-stress checkpoint pathway. Mol Cell Biol. 2003; 23:8902–8912. [PubMed: 14612427]

Zhu Y, Poyurovsky MV, Li Y, Biderman L, Stahl J, Jacq X, Prives C. Ribosomal protein S7 is both a regulator and a substrate of MDM2. Mol Cell. 2009; 35:316–326. [PubMed: 19683495]

Zindy F, Eischen CM, Randle DH, Kamijo T, Cleveland JL, Sherr CJ, Roussel MF. Myc signaling via the ARF tumor suppressor regulates p53-dependent apoptosis and immortalization. Genes & Dev. 1998; 12:2424–2433. [PubMed: 9694806]

Highlights

- Mdm2 central zinc finger is essential for interaction with ribosomal proteins (RP)
- RP-Mdm2 interaction is essential for p53's response to abnormal ribosome biogenesis
- RP-Mdm2 interaction is required for preventing c-Myc induced lymphomagenesis
- RP-Mdm2-p53 pathway acts independent of ARF-Mdm2-p53 pathway against oncogenic c-Myc

Significance

Several ribosomal proteins (RPs) have been shown to interact with and inhibit the E3 ligase function of Mdm2, thereby activating p53. The physiological significance of these interactions, however, has not been established *in vivo*. The $Mdm2^{C305F}$ knockin mouse model provides *in vivo* evidence for a prevailing p53 checkpoint mediated by RP-Mdm2 interaction that monitors the integrity of ribosome biogenesis and activates p53 when this process goes awry. The study presented here also establishes the RP-Mdm2-p53 pathway as an important barrier, parallel to the p19Arf-Mdm2-p53 signaling, for defending against oncogenic c-Myc-induced tumorigenesis.

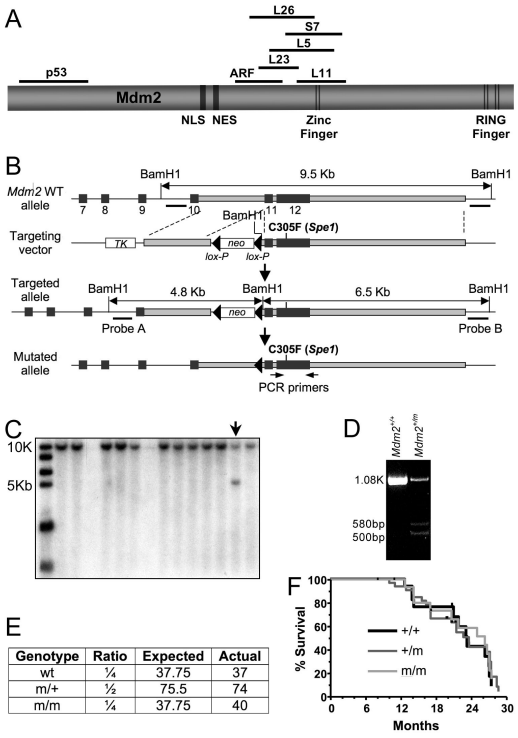

Genotype	Ratio	Expected	Actual
wt	¼	37.75	37
m/+	½	75.5	74
m/m	¼	37.75	40

Figure 1. Generation and analysis of *Mdm2*^{C305F} knockin mice

(A) A diagram of Mdm2 protein and approximate binding domains for p53, ARF, and several ribosomal proteins.

(B) Schematic representation of *Mdm2*^{C305F} targeting strategy. Exons 7-12 of *Mdm2* are shown in black boxes. The targeting vector contains negative selection marker thymidine kinase (*TK*) and positive selection marker neomycin resistant gene (*neo*). Two *loxP* sites are shown as triangles.

(C) Southern blot analysis was used to screen ES clones for the targeted allele. *BamH1* digestion generates a 9.5 kb fragment from the wild type allele. The targeted allele gives rise to two *BamH1* fragments of 4.8 kb and 6.5 kb, respectively.

(D) DNA from ES cells positive for the recombined allele identified was analyzed for the presence of *Mdm2*^{C305F} mutation by PCR amplification and *Spe1* digestion.

(E) Shown are expected and observed birth ratios from a total of 151 mice obtained from *Mdm2*$^{+/m}$ intercross.

(F) Kaplan-Mierer survival curve for *Mdm2*$^{+/+}$ (+/+), *Mdm2*$^{+/C305F}$ (+/m) *and* *Mdm2*$^{C305F/C305F}$ (m/m) mice are shown.

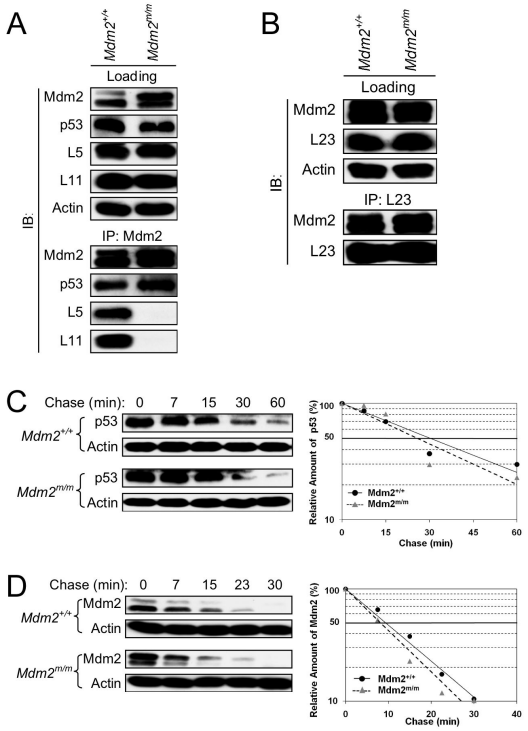

Figure 2. Characterization of Mdm2^{C305F} mutant protein

(A) *Mdm2*$^{+/+}$ and *Mdm2*$^{m/m}$ MEFs were treated with 5 nM Act D and lysates were immunoprecipitated (IP) with anti-Mdm2 antibody and immunoblotted (IB) for Mdm2, p53, L5 and L11 as indicated. Loading represents 5% of total lysate used for IP.

(B) MEFs were treated as in (A) and lysates were analyzed as indicated.

(C) Half-life of p53 in *Mdm2*$^{+/+}$ and *Mdm2*$^{m/m}$ MEFs. Half-life assay was carried out using early passage (P1) MEFs treated with cycloheximide (50 μg/ml) and harvested with SDS lysis buffer at the indicated time points. Relative amount of p53 was quantified by densitometry, normalized to Actin and plotted.

(D) Half-life of Mdm2 and Mdm2^{C305F}. MEFs were treated and analyzed as in (C) for Mdm2.

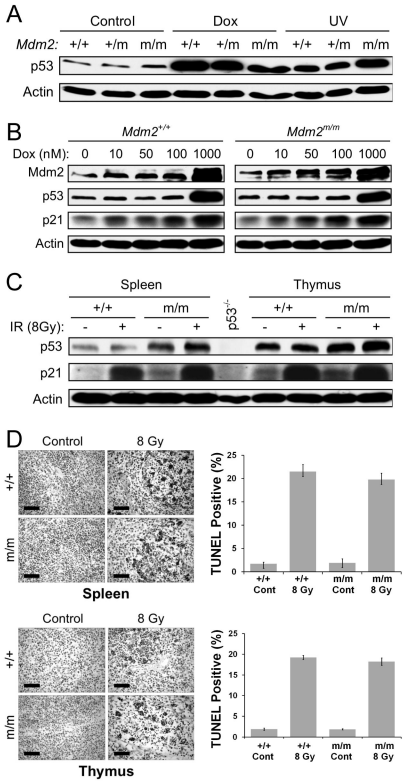

Figure 3. *Mdm2*^{C305F} mice retain intact p53 response to DNA damage

(A) *Mdm2*$^{+/+}$, *Mdm2*$^{m/+}$ and *Mdm2*$^{m/m}$ MEFs were mock treated (Control) or treated with 1 μM doxorubicin (Dox) or 50 J/m^2 of ultraviolet C (UV). The cells were harvested 18 hours post treatment and immunoblotted for p53 and Actin.

(B) *Mdm2*$^{+/+}$ and *Mdm2*$^{m/m}$ MEFs were treated with increasing dosage of Dox for 18 hrs. Cell extracts were analyzed for p53, p21 and Mdm2.

(C) Induction of p21 in spleen and thymus after γ-irradiation. Spleen and thymus were harvested from *Mdm2*$^{+/+}$ and *Mdm2*$^{m/m}$ mice 18 hours after 8-Gy whole body γ-irradiation. Protein extracts were assayed for protein levels of p53, p21, and Actin. Spleen protein extract from a *p53*$^{-/-}$ mouse was used as a negative control.

(D) Apoptotic response to whole body γ-irradiation. The level of apoptosis in spleen and thymus was determined by TUNEL assay, carried out on paraffin embedded tissues from mice 18 hours after receiving 8-Gy of whole body γ-irradiation. The percentage of TUNEL positive cells was quantified and averaged from three identically treated mice. Scale bars represent 75 μm. Error bars in all cases represent ± SD.

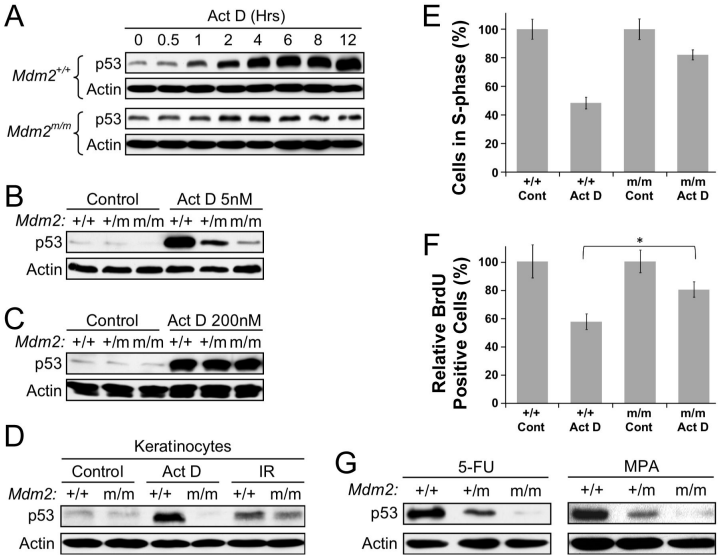

Figure 4. *Mdm2*^{C305F} mice demonstrate attenuated p53 response to ribosome biogenesis stress

(A) MEFs were treated with 5 nM Act D and harvested at indicated time points. Cell lysates were immunoblotted for p53 and Actin.

(B) *Mdm2*$^{+/+}$, *Mdm2*$^{+/m}$ and *Mdm2*$^{m/m}$ MEFs were either mock treated or treated with 5 nM Act D for 12 hours before harvesting for western blot analysis.

(C) p53 response to a DNA damaging dosage of Act D in *Mdm2*$^{m/m}$ MEFs. MEFs were treated with 200 nM Act D for 12 hours and analyzed for p53.

(D) Mouse dorsal skins were treated topically with 200 μl of acetone (Control) or Act D (1 μg/200 μl acetone). Protein lysates were prepared from snap frozen skin collected 18 hours after the treatment by epidermal scrapes and analyzed for p53. As a positive control, dorsal skins were treated with acetone and followed immediately by whole body 8-Gy γ-irradiation (IR), and the skin cells were collected 18 hours after the treatment.

(E) Early passage MEFs were either mock treated or treated with 5 nM Act D for 18 hours. Cell cycle distribution was determined by flow cytometry using propidium iodide (PI) staining. Samples were run in triplicate with a minimum of 15,000 cells analyzed for each treatment.

(F) BrdU incorporation analysis in *Mdm2*$^{m/m}$ keratinocytes. Mouse dorsal skins were treated as in (D) and fixed in formalin 18 hours post treatment. BrdU incorporation was determined by immunohistochemistry. For quantification, BrdU positive interfollicular basal keratinocytes from 15 representative 200 μm fields were counted. Three mice were used for each group. Asterisk indicates *P* value of < 0.01 determined by Tukey's multiple comparison tests.

(G) p53 response to 5-FU and MPA. MEFs were treated with 1 μM 5-FU or 2 μM MPA for 12 hours and assessed for p53 by western blotting.

Error bars in all cases represent ± SD.

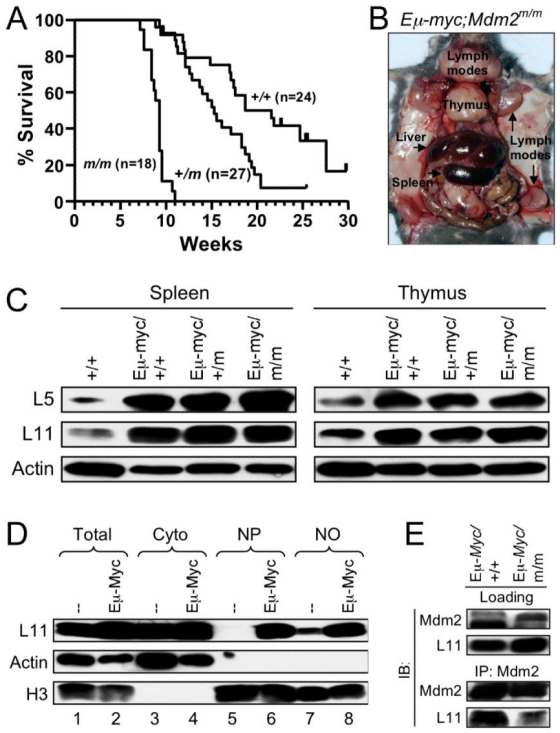

Figure 5. Myc-induced lymphomagenesis is accelerated by Mdm2^{C305F} mutation

(A) Survival of Eμ-*Myc* transgenic mice. Kaplan-Mierer survival curve shows a median survival of 20, 15, and 9 weeks for Eμ-*Myc;Mdm2*$^{+/+}$ (+/+, n= 24), Eμ-*Myc;Mdm2*$^{+/m}$ (+/m, n= 27) and Eμ-*Myc;Mdm2*$^{m/m}$ (m/m, n= 18) mice, respectively.

(B) Lymphoma onset in Eμ-*Myc;Mdm2*$^{m/m}$ mice. Image shows dissection of a 58-day old Eμ-*Myc;Mdm2*$^{m/m}$ mouse with typical enlargement of liver, spleen, thymus and lymph nodes, including enlargement of Peyer's patches and mesenteric lymph nodes.

(C) Extracts from spleen and thymus of wild type (+/+) and tumor bearing Eμ-*Myc* transgenic mice were analyzed for L5 and L11.

(D) Accumulation of L11 in nucleus in Eμ-*Myc* transgenic mouse splenocytes. Lysates of splenocytes from wild type and non-tumor bearing Eμ-*Myc* transgenic mice were subjected to fractionation as described in Experimental Procedures. The total (Total), cytoplasmic (Cyto), nucleoplasmic (NP), and nucleolar (NO) fractions were isolated and analyzed for L11. Actin (cytoplasmic) and Histone H3 (nuclear) were used as fractionation markers.

(E) L11-Mdm2 binding in Eμ-*Myc* transgenic splenocytes. Lysates from spleens of 4-week-old, non-tumor bearing mice were immunoprecipitated with anti-Mdm2 antibody and immunoblotted as indicated. Loading represents 5% of total lysate used for IP.

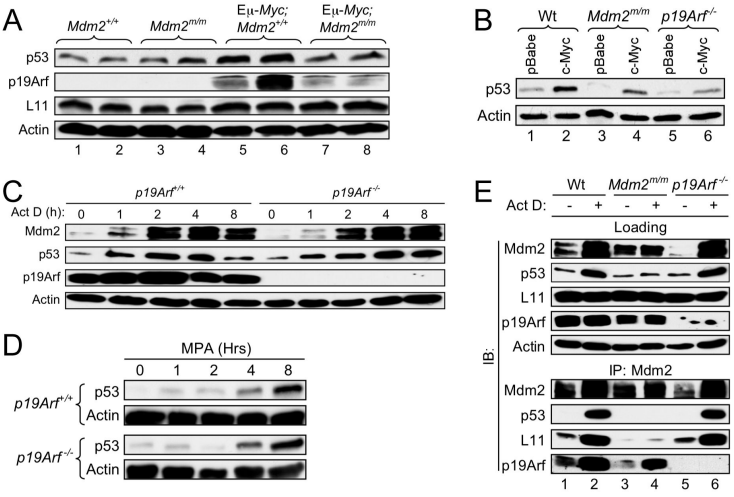

Figure 6. p19Arf is dispensable for p53 response to nucleolar stress

(A) Oncogenic c-Myc induction of p53 in $Mdm2^{C305F}$ mice. Extracts from spleens of 4-week-old, non-tumor bearing Eμ-*Myc;Mdm2*$^{+/+}$ and Eμ-*Myc;Mdm2*$^{m/m}$ transgenics as well as from their non-transgenic counterparts were analyzed for p53, p19Arf, and L11. Two mice are used in each group.

(B) Myc induction of p53 in the absence of p19Arf. Early passage wild type, *Mdm2*$^{m/m}$ and *p19Arf*$^{-/-}$ MEFs were infected with retrovirus expressing either pBabe vector or pBabe-c-Myc, selected by puromycin for 3 days, then allowed to recover for 48 hours before harvesting for western analysis.

(C) Early passage wild type and *p19Arf*$^{-/-}$ MEFs were treated with 5 nM Act D and harvested at the indicated time points. Cell lysates were analyzed for indicated proteins.

(D) p53 response to MPA in *p19Arf*$^{-/-}$ MEFs. Early passage wild type and *p19Arf*$^{-/-}$ MEFs were treated with 2 μM MPA for 12 hours, then harvested and analyzed for p53.

(E) L11-Mdm2 and p19Arf-Mdm2 interaction in Act D treated MEFs. Early passage wild type, *Mdm2*$^{m/m}$ and *p19Arf*$^{-/-}$ MEFs were treated with 5 nM Act D for 4 hours. Cell lysates were immunoprecipitated with anti-Mdm2 antibody and immunoblotted as indicated. Loading represents 5% of total lysate used for IP.

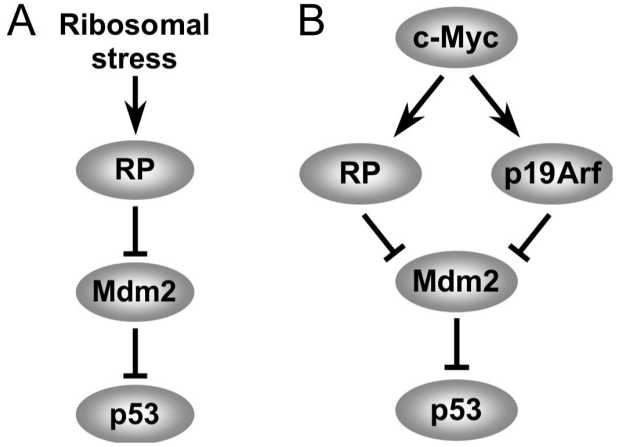

Figure 7. Models for RP-Mdm2-p53 signaling in response to ribosomal stress and oncogenic c-Myc

(A) In response to ribosomal stress several ribosomal proteins, including L11 and L5, bind Mdm2 and inhibit its E3 ligase function, leading to stabilization and activation of p53.

(B) Oncogenic c-Myc induces high expression of both p19Arf and ribosomal proteins. The RP-Mdm2-p53 and p19Arf-Mdm2-p53 represent two parallel signaling pathways in response to oncogenic c-Myc stimulation.